

Synthesis and characterization of vincristine loaded folic acid–chitosan conjugated nanoparticles

Raj Kumar Salar *, Naresh Kumar

Department of Biotechnology, Chaudhary Devi Lal University, Sirsa 125055, Haryana, India

Received 7 June 2016; received in revised form 6 October 2016; accepted 10 October 2016

Available online 9 November 2016

Abstract

Vincristine is an anticancer drug used to treat different types of cancer. However, vincristine has been reported to become resistant against some cancer such as small cell lung cancer cell lines due to decreased uptake, increased drug efflux etc. To increase the uptake, vincristine loaded folic acid–chitosan conjugated nanoparticles were synthesized using ionic gelation method at pH 2.5. ¹H-NMR confirmed conjugation of folic acid with chitosan. Blank folic acid–chitosan conjugated nanoparticles had an average size of 897.5 ± 0.90 nm, a polydispersity index of 0.738 ± 0.30 and zeta potential of $+11.2 \pm 0.43$ mV and found to increase in vincristine loaded folic acid–chitosan nanoparticles at different formulations due to loading of vincristine in folic acid–chitosan conjugated nanoparticles. Fourier Transform Infrared Spectroscopy (FTIR) revealed different functional groups and loading of vincristine in chitosan nanoparticles. X-ray diffraction (XRD) was performed to confirm the crystalline nature of the drug after loading and face centered cubic (FCC) structure of nanoparticles. *In vitro* drug release study showed slow and sustained release of vincristine in phosphate buffered saline at pH 6.7. Scanning Electron Microscopy (SEM) revealed spherical and rough surface of nanoparticles. Transmission Electron Microscopy (TEM) confirmed loading of vincristine and size range of nanoparticles from 4.24 to 300 nm. Spectrophotometric analysis depicted maximum encapsulation efficiency and loading capacity of 81.25% and 10.31%, respectively. Since cancer cells express folate receptors on their surface, these vincristine loaded folic acid–chitosan conjugated nanoparticles could be used for targeted delivery against resistant cancer with some modifications. © 2016 Tomsk Polytechnic University. Production and hosting by Elsevier B.V. This is an open access article under the CC BY-NC-ND license (<http://creativecommons.org/licenses/by-nc-nd/4.0/>).

Keywords: Chitosan; Folic acid; Nanoparticles; Vincristine

1. Introduction

A variety of natural molecules either alone or in combination with radiation therapy have shown their anti-cancerous effects [1]. Of these, vincristine is one of the vinca alkaloids which acts as antineoplastic agent and is used to treat different types of cancers such as breast cancer, Hodgkin's disease, Kaposi's sarcoma, testicular cancer etc [2]. Vincristine binds to tubulin and prevents its polymerization leading to blocking of mitosis [3,4]. However, researchers reported resistance of vincristine uptake by some cancer cell lines such as human lung-cancer PC-9 sub line [5], human gastric carcinoma cell line SGC7901 [6], human cancer KB cell VJ-300 [7] etc.

In recent years, nanomedicine has emerged as a ray of hope to overcome such type of resistances. Attempts have been

made by researchers to increase solubility and bioavailability of vincristine by encapsulating in biodegradable polymeric nanoparticles [8,9]. Among various polymers, chitosan has attracted attention of researchers due to its unique property as drug carrier. Chitosan is a natural polysaccharide, obtained from chitin of arthropods like shrimp and crab [10]. Chitosan is the deacetylated form of chitin (2-amino-2-deoxy-(1–4)-D-glucopyranan) and exhibits excellent properties such as biodegradability, biocompatibility and antimicrobial activity [11]. Chitosan nanoparticles are widely used to deliver hydrophobic drugs, vitamins, proteins, nutrients and phenolics into the biological systems and are stable and less toxic [12,13]. It requires simple methods for preparation of anticancer drug loaded chitosan nanoparticles thereby improving its versatility as drug delivery agent [14]. When chitosan comes in contact with polyanions such as sodium tripolyphosphate, it forms inter and intramolecular cross-linkages through ionic gelation for encapsulation of drugs [15]. Various ligands such as folic acid can be attached to chitosan by different

* Corresponding author. Department of Biotechnology, Chaudhary Devi Lal University, Sirsa 125055, Haryana, India.

E-mail address: rajsalar@rediffmail.com (R.K. Salar).

methods so that these chitosan nanoparticles become target specific.

In the present investigation, vincristine loaded folic acid–chitosan conjugated nanoparticles were synthesized in different ratios. Physicochemical properties such as average particle size, polydispersity index, zeta potential, FTIR, XRD, SEM, TEM etc. were measured for blank and vincristine loaded nanoparticles.

2. Materials and methods

2.1. Chemicals

Low molecular weight chitosan ($\geq 75\%$ deacetylation degree), *N,N'*-Dicyclohexylcarbodiimide (DCC), Dimethyl sulphoxide (DMSO), *N*-Hydroxysuccinimide, Pure (NHS), Phosphate buffered saline (Dulbecco A), Folic acid, Acetate buffer (pH 5.6), Triethylamine and Dialysis Tubing (LA653) were purchased from HiMedia Laboratories, India. Sodium tripolyphosphate (85%) was purchased from Sigma Aldrich. All other chemicals and reagents used in the study were of laboratory grades.

2.2. Synthesis of *N*-Hydroxysuccinimide ester of folic acid

N-Hydroxysuccinimide ester of folic acid was synthesized according to previously reported method with slight modifications [16]. Briefly, 1.5 g folic acid was dissolved in 25 ml dimethyl sulfoxide and added 2 ml *N*-Hydroxysuccinimide (1.0 M) and *N,N'*-dicyclohexylcarbodiimide (1.0 M) each followed by addition of 2.0 ml triethylamine. The reaction was allowed to proceed for 17 h under stirring in the dark in a shaker. The dark pale yellow colored by-product dicyclohexylurea was removed by filtration using filter paper (11 μm). Filtered NHS ester of folic acid was washed with 30% acetone and used for further research.

2.3. Synthesis of folic acid–chitosan conjugate

Folic acid was conjugated with chitosan by using the method of Ji et al. [17] with some modifications. Briefly, 45 mg chitosan was dissolved in 15 ml acetate buffer (pH 5.6). 1 g *N*-Hydroxysuccinimide ester of folic acid was separately dissolved in 15 ml Dimethyl Sulphoxide and added to chitosan solution drop wise. Mixture was stirred at 30 °C in the dark for 20 h on a laboratory shaker resulting in the formation of folic acid–chitosan conjugate. The solution was filtered using filter paper (11 μm) and conjugates were transferred to 2.0 ml microcentrifuge vial and stored in refrigerator for further use. The $^1\text{H-NMR}$ spectra of chitosan and folic acid–chitosan conjugate were recorded on a 400 MHz FT NMR spectrometer (Avance II, Bruker) using D_2O as a solvent.

2.4. Synthesis of blank and vincristine loaded chitosan nanoparticles

Blank and vincristine loaded folic acid–chitosan conjugated nanoparticles were synthesized by ionic cross-linking with sodium tripolyphosphate (TPP) using a previously reported method [18] with minor modifications. Folic acid–chitosan conjugate solution (0.2%, w/v, pH 2.5) was prepared using

acetic acid (2%, v/v) at room temperature. Sodium tripolyphosphate (0.5%, w/v) solution was prepared using distilled water. For the preparation of blank nanoparticles, 100 ml folic acid–chitosan conjugate solution was taken in a flask and 20 ml sodium tripolyphosphate (1:5 ratios) solution was added to it drop wise till the formation of nanoparticles suspension and stirred for 30 minutes on a magnetic stirrer at room temperature. For the synthesis of vincristine loaded nanoparticles, aqueous solution of vincristine (1 mg/10 ml, pH 4.77) was prepared separately. Keeping folic acid–chitosan conjugate (25 ml) and sodium tripolyphosphate (5 ml) volume constant varying volumes of vincristine (100 μl , 200 μl , 300 μl , 400 μl) were used for the synthesis of different ratios of nanoparticles, i.e., 1:25, 2:25, 3:25 and 4:25, respectively and allowing the solution to stir for 30 minutes on a magnetic stirrer at room temperature. Nanoparticles suspension for blank and vincristine loaded folic acid–chitosan conjugated nanoparticles was centrifuged at 16,000 rpm for 30 minutes for separating the nanoparticles from the solution for further characterization.

2.5. Encapsulation efficiency and actual drug loading

For determination of the encapsulation efficiency (%) and actual drug loading (%), vincristine loaded folic acid–chitosan conjugated nanoparticles were centrifuged at 16,000 rpm for 30 min. The content of free vincristine in the supernatant was determined by UV spectrophotometer at 220 nm using supernatant of their corresponding blank nanoparticles without loaded drugs as basic correction. Encapsulation efficiency and drug loading were calculated by the following equations:

$$\text{Encapsulation efficiency (\%)} = \frac{(\text{Drug})_{\text{tot}} - (\text{Drug})_{\text{free}}}{(\text{Drug})_{\text{tot}}} \times 100$$

Actual drug loading (% w/w)

$$= \frac{\text{Mass of vincristine in chitosan nanoparticles}}{\text{Mass of chitosan nanoparticles recovered}} \times 100.$$

2.6. Storage stability of nanoparticles

Fresh vincristine loaded folic acid–chitosan conjugated nanodispersion (200 μl) was separately added to 50 ml of phosphate buffer saline solutions with different pH (5, 6, 6.7, 7.2 and 7.7). Samples in all ratios (1:25, 2:25, 3:25, 4:25) were also stored in deionized water to calculate relative light transmittance (Ti/T %). The samples were stored at room temperature. The light transmittance was measured at 220 nm by UV spectrophotometer at scheduled time intervals [19]. Relative light transmittance was calculated as per the following equation:

$$\text{Ti/T \%} = \frac{\text{Transmittance of vincristine loaded folic acid} - \text{chitosan conjugated nanoparticles at each pH}}{\text{Transmittance at deionized water}} \times 100$$

2.7. Characterization of blank and vincristine loaded folic acid–chitosan nanoparticles

Blank and vincristine loaded folic acid–chitosan conjugated nanoparticles were characterized using different techniques.

2.7.1. Average size, polydispersity index and zeta potential

Average size, polydispersity index and zeta potential of blank and vincristine loaded folic acid–chitosan conjugated nanoparticles were determined by dynamic laser scattering (DLS) technique using Malvern Zetasizer Nanoseries Nanos ZS90 (Malvern Instruments, UK). Before measurement, the nanoparticles (50 μl) were dispersed in water (950 μl) to make a total volume of 1 ml and readings were obtained at 25 $^{\circ}\text{C}$.

2.7.2. Fourier transformation infrared spectroscopy (FTIR)

The Fourier transform infrared (FTIR) spectra of blank nanoparticles, vincristine and vincristine loaded chitosan nanoparticles of different ratios (1:25, 2:25, 3:25 and 4:25) were analyzed by Perkin Elmer-Spectrum RX-IFTIR. Scanning range was selected from 4000 cm^{-1} to 400 cm^{-1} and resolution was 1 cm^{-1} .

2.7.3. X-ray diffraction (XRD)

X-ray diffraction (XRD) of vincristine loaded folic acid–chitosan nanoparticles of different ratios (1:25, 2:25, 3:25 and 4:25) was analyzed by Panalytical's X'Pert Pro, Netherlands with Cu K-alpha-1 as radiation and nickel metal as beta filter in θ –2 θ configuration.

2.7.4. In vitro release study

The *in vitro* release profile of vincristine from folic acid–chitosan conjugated nanoparticles was determined by dialysis tubing (molecular weight cut off 12,000–14,000) at 37 $^{\circ}\text{C}$. 10 mg of nanoparticles was added to 1 ml phosphate buffered saline (pH 6.7) and poured in a dialysis membrane, dipped in phosphate buffered saline (pH 6.7) in different beakers. The beakers were placed on a laboratory shaker. After definite intervals of time, 1 ml of phosphate buffered saline (pH 6.7) was taken out and same amount of buffer was added. The absorbance of resulting solution was measured at 220 nm to determine the concentration of vincristine in the buffer.

2.7.5. Scanning electron microscopy (SEM)

The morphology of blank and vincristine loaded chitosan nanoparticles was examined by Scanning Electron Microscopy (JEOL Model JSM – 6390LV). Few milliliters of samples were placed in aluminum stubs and then coated with platinum. The SEM images were taken with an acceleration voltage of 15 kV.

2.7.6. Transmission electron microscopy (TEM)

Size of blank and vincristine loaded FA–CS nanoparticles was examined by Transmission Electron Microscopy (Jeol/JEM 2100) with an operating voltage of 200 kV. Loading of vincristine in chitosan nanoparticles was also confirmed by TEM.

3. Results and discussion

3.1. Synthesis of *N*-Hydroxysuccinimide ester of folic acid and folic acid–chitosan conjugate

N-Hydroxysuccinimide is an activating agent of carboxylic acid which activated carboxylic group of folic acid during 17 h stirring in the dark. *N*-Hydroxysuccinimide reacted with folic acid in the presence of *N,N'*-dicyclohexylcarbodiimide to produce yellow colored dicyclohexylurea confirming the synthesis of

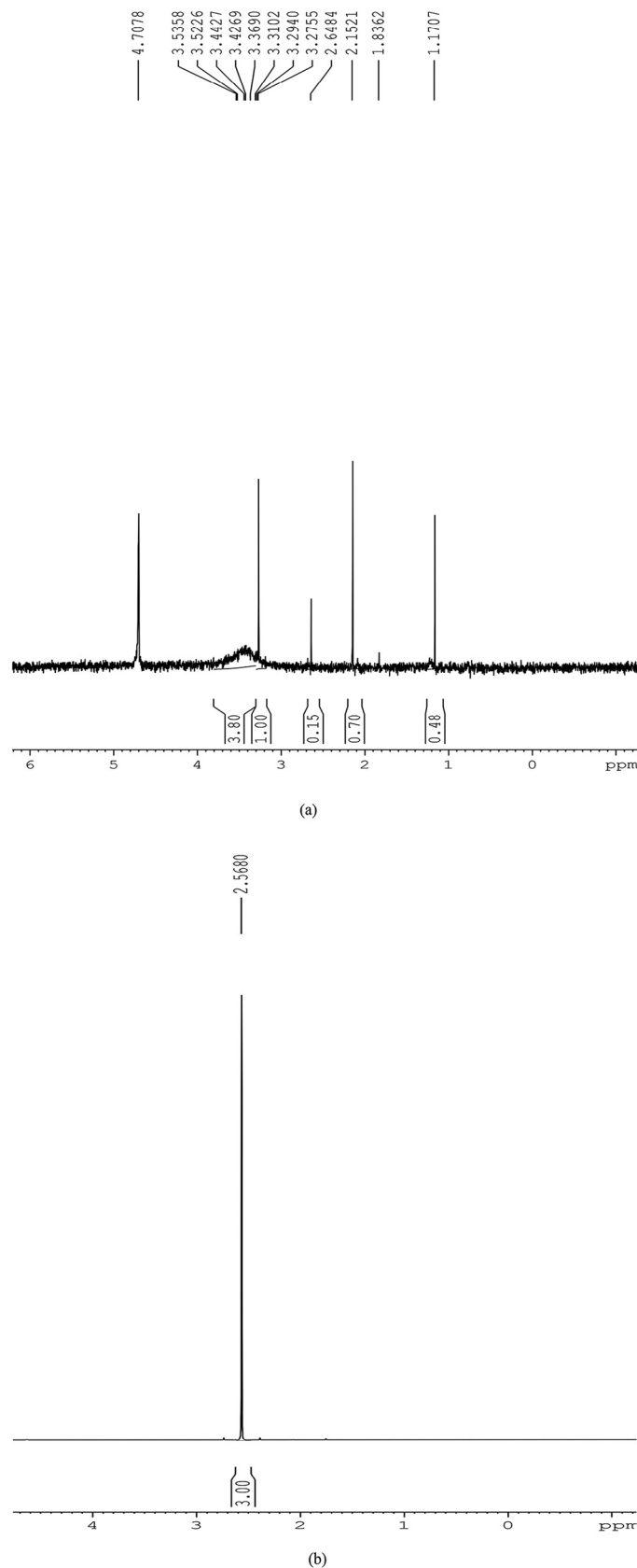


Fig. 1. ^1H NMR spectrum of (a) chitosan and (b) folic acid–chitosan conjugate showing binding of folic acid with chitosan.

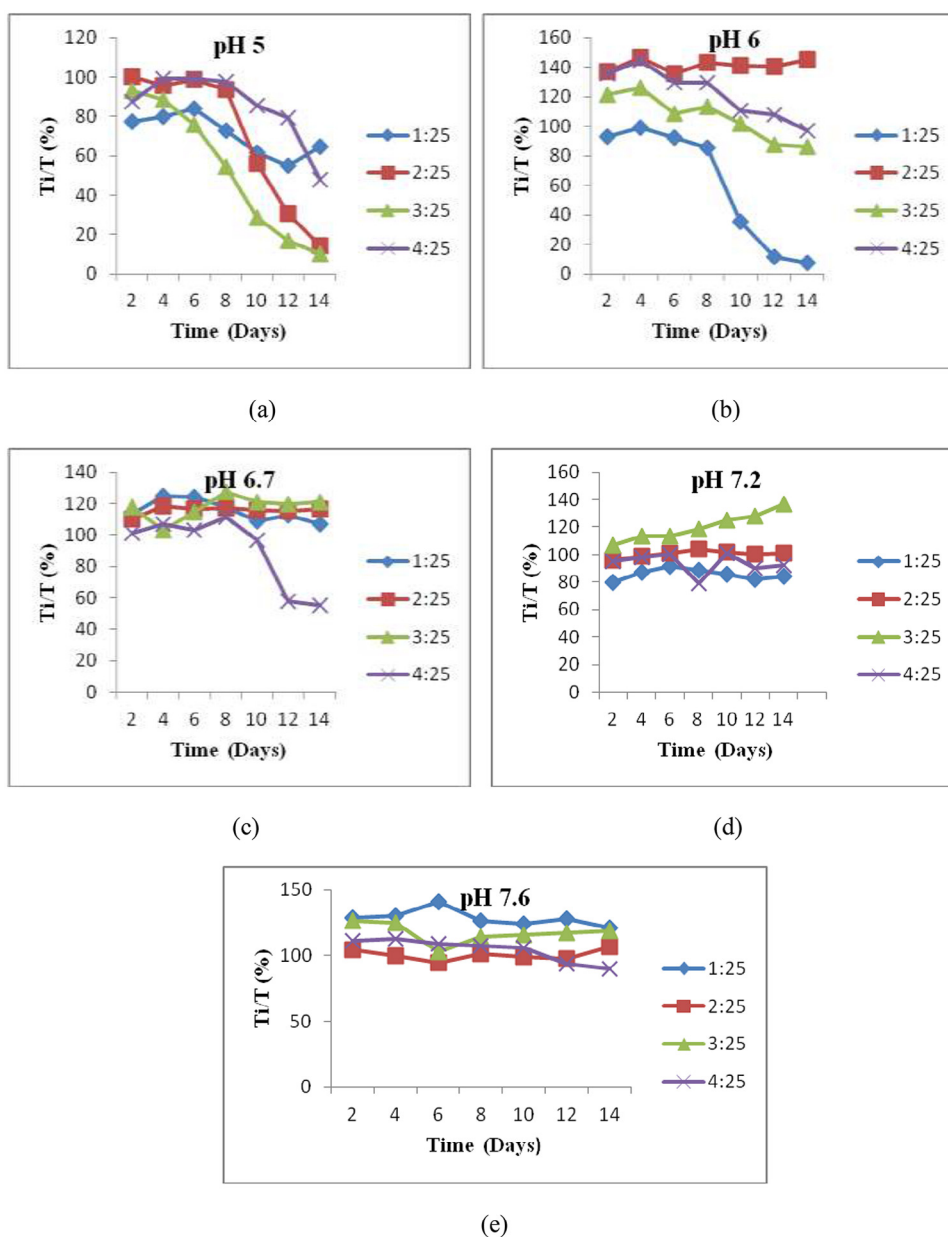


Fig. 2. Relative light transmittance (Ti/T) of vincristine loaded nanoparticles: (a) pH 5, (b) pH 6, (c) pH 6.7, (d) pH 7.2, (e) pH 7.6.

N-Hydroxysuccinimide ester of folic acid. Further, folic acid was conjugated to chitosan following the *N*-Hydroxysuccinimide ester of folic acid reaction to get folic acid–chitosan conjugate. ¹H NMR proved conjugation of folic acid to chitosan. Two carboxylic groups (-COOH) are present at the end position of folic acid and it has been supported by literature that γ -COOH is more reactive [20]. Folic acid–chitosan conjugate was synthesized by the formation of amide bond between activated *N*-Hydroxysuccinimide ester of folic acid and the primary amine groups of chitosan. The structure of chitosan and folic acid–chitosan conjugate by ¹H-NMR spectroscopy is shown in Fig. 1 and b. The peaks at 2.6484 ppm were due to acetamino group CH₃ and CH peak appeared at 3.4269–3.5358 ppm due to carbons 3, 4, 5, and 6 of glucosamine ring of chitosan (Fig.

1a). Appearance of the peculiar signals at 2.5680 ppm was due to the formation of amide bond through reaction between activated folic acid ester and the primary amine groups of chitosan as shown in Fig. 1b and corresponds to the folic acid proton from the H22 [21]. ¹H-NMR spectroscopic data were analyzed using online software [22]. Similar results were obtained by Ji et al. [17] while grafting folic acid to chitosan for target specific delivery of methotrexate.

3.2. Blank and vincristine loaded chitosan nanoparticles

The folic acid–chitosan conjugated nanoparticles synthesis occurred due to ionic interaction between positively charged free protonated amino group ($-\text{NH}_3^+$) of the folic acid–chitosan

Table 1
Encapsulation efficiency (%) and vincristine loading (%) of chitosan nanoparticles.

Sr. No.	Ratios	Encapsulation efficiency (%)	Loading of vincristine in chitosan nanoparticles (% w/w)
1.	1:25	20 ± 0.58	0.6 ± 0.15
2.	2:25	65 ± 0.53	3.83 ± 0.19
3.	3:25	66.6 ± 0.23	6.06 ± 0.97
4.	4:25	81.25 ± 0.43	10.31 ± 0.76

conjugate and negatively charged sodium tripolyphosphate [17]. However, size distribution of nanoparticles depends upon the ratio of chitosan and sodium tripolyphosphate which affects biological properties and their role [23]. Different ratios of vincristine loaded folic acid–chitosan nanoparticles were synthesized. 5-Fluorouracil loaded chitosan nanoparticles by ionic gelation method have been reported [24]. Earlier, ferulic acid has been loaded in chitosan nanoparticles by ionic gelation to check anticancer activity against ME-180 human cervical cancer cell lines [25].

3.3. Encapsulation efficiency and drug loading

Vincristine was loaded in chitosan nanoparticles due to ionic reaction. As shown in Table 1, encapsulation efficiency (%) for

1:25, 2:25, 3:25 and 4:25 was 20 ± 0.58 , 65 ± 0.53 , 66.6 ± 0.23 and 81.25 ± 0.43 , respectively. Maximum encapsulation was reported in 4:25 ratio ($81.25 \pm 0.43\%$) because concentration of vincristine was higher as compared to other ratios. However, after crossing maximum loading capacity, more drugs could be wasted during the synthesis process [26]. Drug loading capacity (%) was 0.6 ± 0.15 , 3.83 ± 0.19 , 6.06 ± 0.97 and 10.31 ± 0.76 for 1:25, 2:25, 3:25 and 4:25 ratios, respectively. Drug loading was found to be maximum (10.31%) for 4:25 ratio (Table 1). Previous studies [25] have shown that ferulic acid loaded chitosan nanoparticles with varying concentrations (1, 5, 10, 20, 40, 80, 40 μM) of ferulic acid, chitosan and sodium tripolyphosphate have been synthesized. Maximum encapsulation efficiency of ferulic acid ($63.0 \pm 2.20\%$) was achieved at 40 μM . Similarly, maximum loading capacity ($32.9 \pm 2.1\%$) was found at 80 μM concentration of ferulic acid [25]. Mitoxantrone, an anticancer drug, has been loaded in folic acid–chitosan conjugated nanoparticles in different ratios, i.e. 1:1, 1:2, 1:3 and 1:4 with respect to mitoxantrone and folic acid–chitosan conjugate. It was reported that when mitoxantrone vs folic acid–chitosan conjugate ratio was increased from 1:4 to 1:1, the loading capacity was also enhanced from 12.2% to 32.3%, but the highest encapsulation efficiency (77.5%) was observed when ratio of mitoxantrone vs folic acid–chitosan conjugate was 1:3 [27].

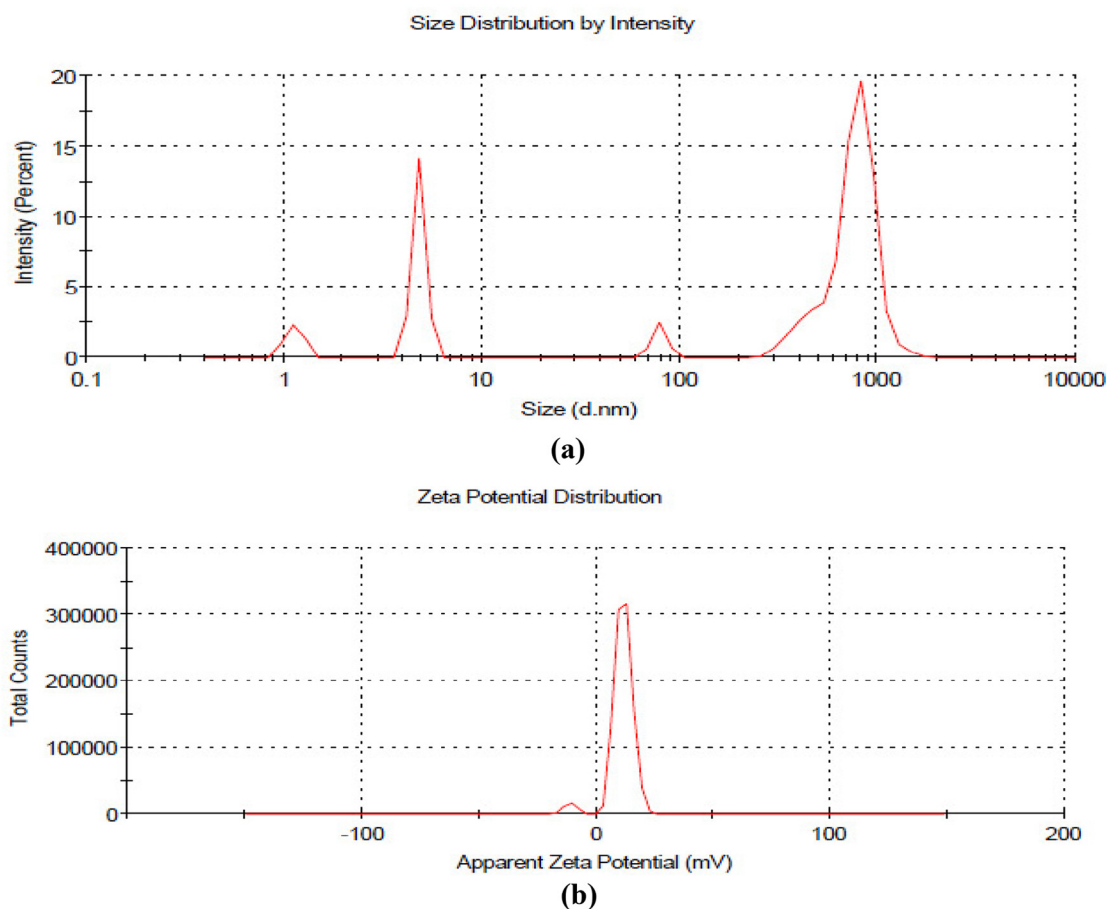


Fig. 3. Blank folic acid–chitosan conjugated nanoparticles. (a) Average particle size and polydispersity index (b) zeta potential.

3.4. Storage stability of nanoparticles

Fig. 2 shows stability of nanoparticles at different pH up to 14 days as monitored by relative light transmittance, i.e., Ti/T %. There was no significant change in the turbidity of nanoparticles stored at different pH indicating highly stable nature of nanoparticles. An overview of Fig. 2a indicates that there was a change in Ti/T % for 1:25, 2:25, 3:25, and 4:25 with passage of time for pH 5. It reveals that nanoparticles were not stable at pH 5. On the other hand at pH 6, 2:25, 3:25 and 4:25 ratios showed decrease in Ti/T % as compared to 1:25 (Fig. 2b). This confirmed the stability of nanoparticles at 1:25 ratio at pH 6. Further, as shown in Fig. 2c (pH 6.7), only 4:25 ratio showed decrease in relative transmittance whereas 1:25, 2:25 and 3:25 showed minor change confirming nanoparticle stability at pH 6.7. At pH 7.2, all ratios showed minor change in the relative absorbance with passage of time except for 1:25 (Fig. 2d) which indicates stability, whereas all ratios of nanoparticles at pH 7.6 showed constant relative absorbance with passage of time indicating their high stability (Fig. 2e). So it is envisaged that the synthesized nanoparticles were highly stable at pH 7.2 and 7.6 as compared to pH 5, 6 and 6.7. Similar results were also

obtained while monitoring stability of methotrexate in folic acid–chitosan conjugated nanoparticles [17].

3.5. Characterization of blank and vincristine loaded chitosan nanoparticles

3.5.1. Average size, polydispersity index and zeta potential

As shown in Fig. 3a, average size of blank chitosan nanoparticles was 897.5 ± 0.90 nm with major percentage of nanoparticles corresponding to the peak over 100 nm and polydispersity index was 0.738 ± 0.30 . Zeta potential of folic acid–chitosan conjugated nanoparticles was $+11.2 \pm 0.43$ mV (Fig. 3b). Average size of vincristine loaded folic acid–chitosan nanoparticles in the ratio of 1:25 was 1598.13 ± 0.60 nm with 67% peaks of 700.5 nm size, polydispersity index of 0.937 ± 0.11 and zeta potential of $+9.84 \pm 0.51$ mV (Fig. 4a and b). Similarly, vincristine loaded folic acid–chitosan nanoparticles at a ratio of 2:25 showed average size of 2200 ± 0.64 nm having nanoparticles of different percentages with polydispersity index of 0.454 ± 0.26 and zeta potential of $+7.99 \pm 0.92$ mV as shown in Fig. 5a and b. Fig. 6a and b indicates vincristine loaded folic acid–chitosan nanoparticles at a ratio of 3:25 had an

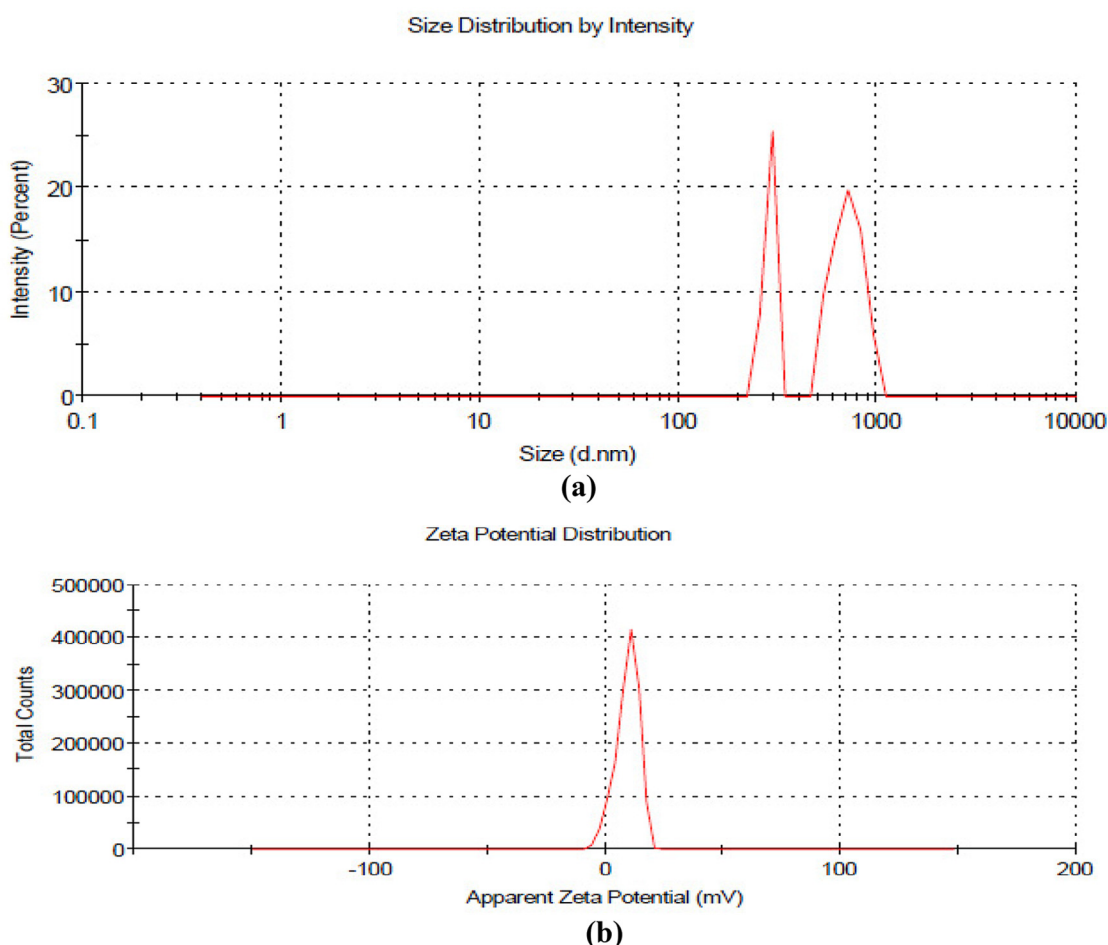


Fig. 4. Vincristine loaded folic acid–chitosan conjugated nanoparticles at a ratio of 1:25. (a) Average particle size and polydispersity index (b) zeta potential.

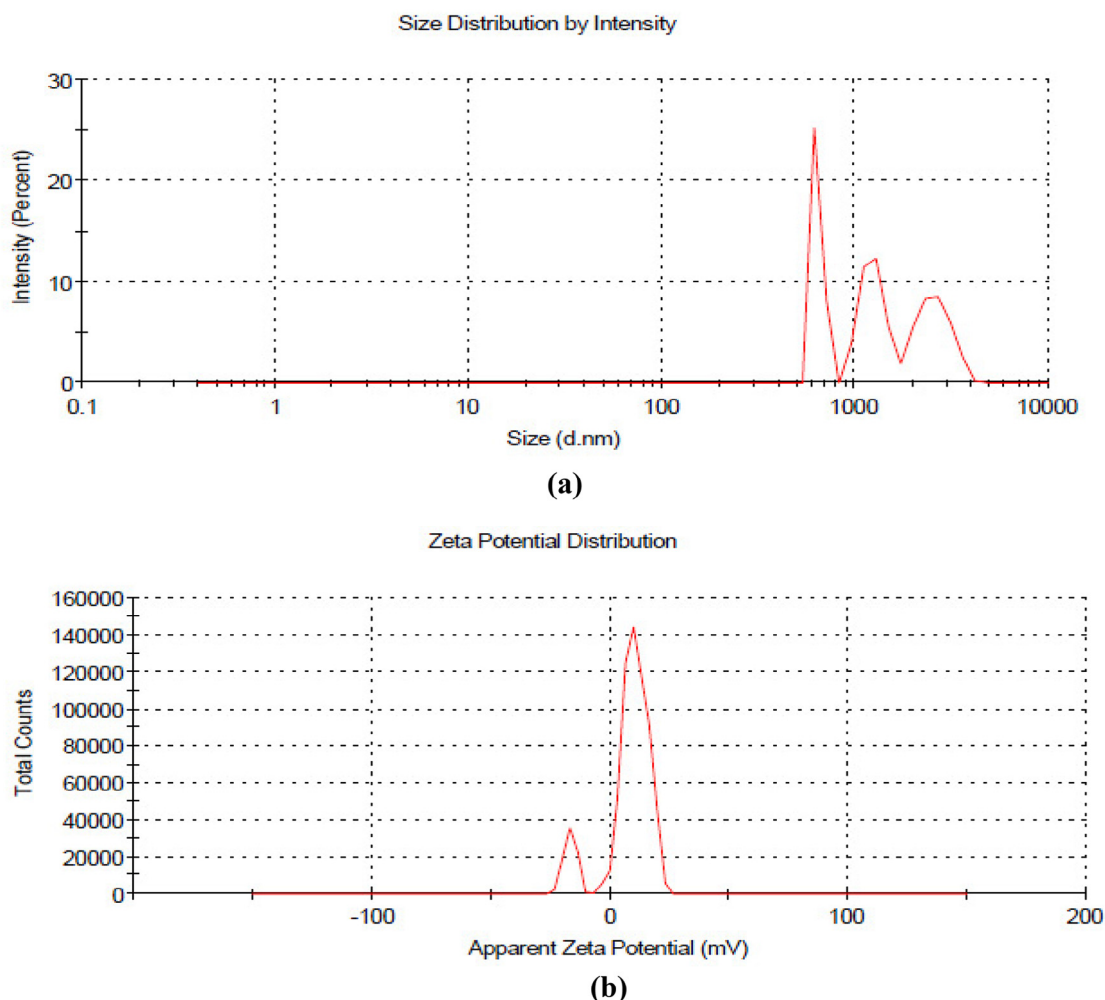


Fig. 5. Vincristine loaded folic acid–chitosan conjugated nanoparticles at a ratio of 2:25. (a) Average particle size and polydispersity index (b) zeta potential.

average size of 2532.33 ± 0.35 nm with 69.8% of 761.3 nm size, polydispersity index of 0.942 ± 0.01 and zeta potential of $+10.5 \pm 0.46$ mV, whereas vincristine loaded folic acid–chitosan nanoparticles at a ratio of 4:25 had an average size of 3812 ± 0.38 nm with 63.2% of 1190 nm size and polydispersity index of 0.703 ± 0.10 . Zeta potential was $+12.6 \pm 0.2$ mV (Fig. 7a and b). This positive zeta potential is useful to cross negatively charged cancer cell membrane. In an earlier study [17] different sized, methotrexate loaded folic acid–chitosan conjugated nanoparticles were synthesized at different pH. At pH 4.0 size, polydispersity index, zeta potential was 316.9 ± 16.9 nm, 0.229 ± 0.034 , 31.48 ± 2.32 ; at pH 4.5, 329.2 ± 13.3 nm, 0.295 ± 0.049 , 29.04 ± 2.29 ; at pH 5.0, 358.2 ± 15.6 nm, 0.224 ± 0.040 , 23.81 ± 1.85 ; at pH 5.5, 394.1 ± 23.0 nm, 0.256 ± 0.032 , 22.84 ± 1.79 respectively.

3.5.2. Fourier transformation infrared spectroscopy (FTIR)

FTIR spectra of blank, vincristine and vincristine loaded folic acid–chitosan conjugated nanoparticles in different ratios are shown in Fig. 8a–f. The blank folic acid–chitosan conjugated

nanoparticles spectrum (Fig. 8a) showed a characteristic peak at 3399.0 cm^{-1} (N–H stretching vibration), which was shifted to 3391.16 cm^{-1} , 3368.11 cm^{-1} , 3399.0 cm^{-1} and 3396.0 cm^{-1} (N–H stretching vibration) in 1:25, 2:25, 3:25 and 4:25 ratios, respectively. Wider peak at 3399 cm^{-1} demonstrated that inter- and intra-molecular actions were enhanced in folic acid–chitosan nanoparticles because of the tripolyphosphoric groups of sodium tripolyphosphate linked with ammonium group of folic acid–chitosan conjugate [28]. Peak at 1643.6 cm^{-1} for blank nanoparticles was due to NH_2 deformation vibration, which indicated the linkage between sodium tripolyphosphate and ammonium ion of the folic acid–chitosan conjugation and it was shifted to 1627.24 cm^{-1} , 1628.18 cm^{-1} , 1639.5 cm^{-1} and 1643.3 cm^{-1} (NH_2 deformation) for 1:25, 2:25, 3:25 and 4:25 ratios, respectively. Such shifting indicated interaction of vincristine with folic acid–chitosan conjugated nanoparticles.

FTIR spectrum of vincristine (Fig. 8b) showed peak at 3410.43 cm^{-1} due to broad O–H stretching vibration. Peaks at 3055.58 cm^{-1} (C–H stretching vibration), 2954.56 cm^{-1} ($-\text{CH}_3$ symmetrical stretching vibration), 2675.62 cm^{-1} (C–H stretching

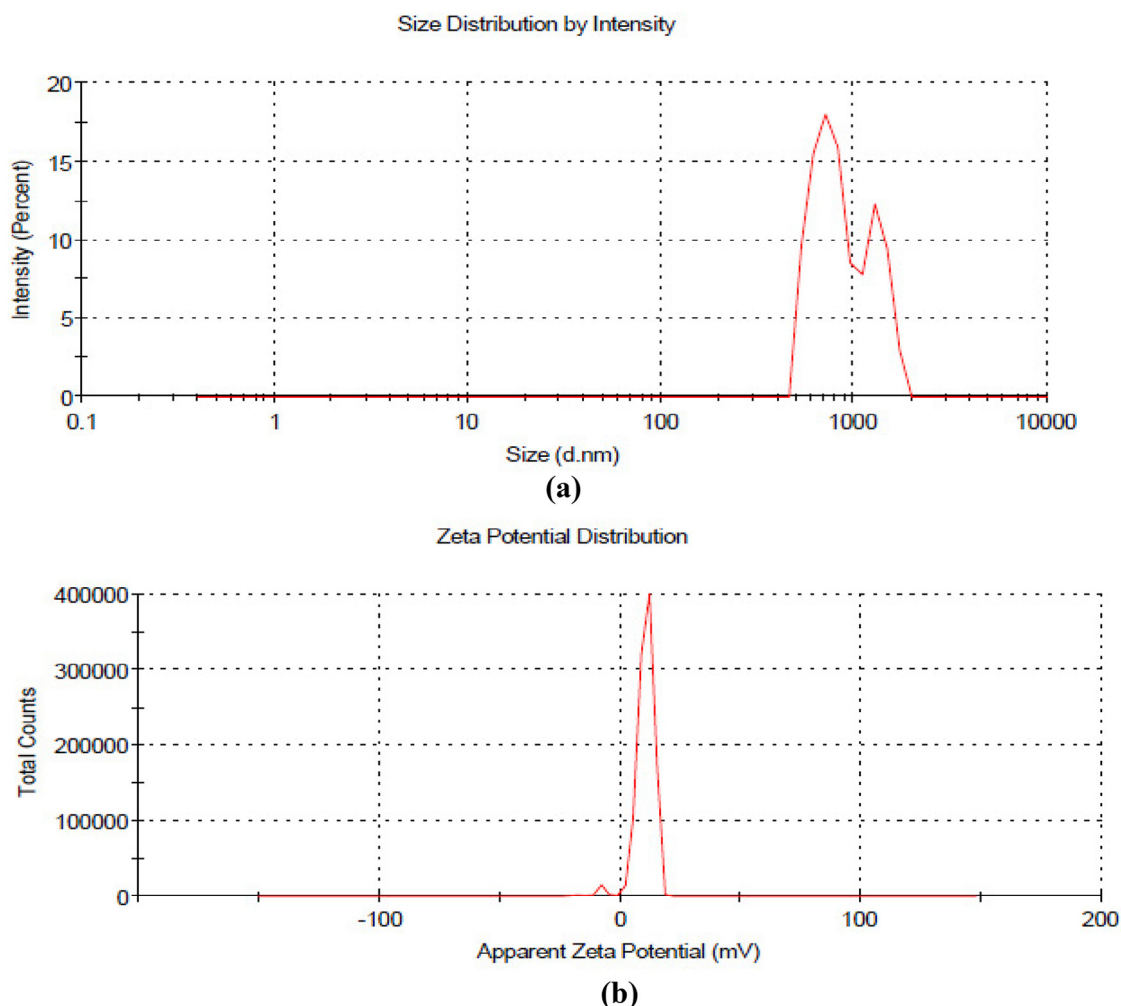


Fig. 6. Vincristine loaded folic acid–chitosan conjugated nanoparticles at a ratio of 3:25. (a) Average particle size and polydispersity index (b) zeta potential.

vibration) and 1747.48 cm^{-1} ($\text{C}-\text{O}$ stretching vibrations) were also observed. Similar peaks were also observed for vincristine loaded folic acid–chitosan conjugated nanoparticles at 2928.30 cm^{-1} (CH_3 symmetrical stretching vibration) and 2849.32 cm^{-1} ($\text{C}-\text{H}$ stretching vibration) for 1:25, 2930.24 cm^{-1} (CH_3 symmetrical stretching vibration) and 2850.27 cm^{-1} ($\text{C}-\text{H}$ stretching vibration) for 2:25, 2954.11 cm^{-1} , 2932.11 cm^{-1} (CH_3 symmetrical stretching vibration) and 2850.15 cm^{-1} ($\text{C}-\text{H}$ stretching vibration) for 3:25 and 2851.13 cm^{-1} ($\text{C}-\text{H}$ stretching vibration) for 4:25, which confirmed vincristine has been loaded in the nanoparticles. Jeevitha and Kanchana [29] also observed shifts in peaks while loading anticancer drug Piceatannol in Chitosan–poly(lactic acid) nanoparticles. These shifts in peaks confirmed the loading of vincristine successfully in folic acid–chitosan conjugated nanoparticles.

3.5.3. X-ray diffraction (XRD)

X-ray diffraction pattern of vincristine loaded folic acid–chitosan conjugated nanoparticles in different ratios is

presented in Fig. 9. One strong peak at 2θ values (8.0674°) was observed for 1:25 ratio which was shifted to 8.0392° , 7.6540° , and 8.0339° for 2:25, 3:25 and 4:25 ratios, respectively. There was also a shift in small peaks (2θ values) from 15.6263° , 17.6045° , 20.5200° , 21.7113° , 22.2702° , 22.7747° , 23.2869° , 23.5219° , 29.1183° for 1:25 ratio to 15.6153° , 17.5764° , 20.3910° , 20.6406° , 21.5972° , 22.1982° , 22.4728° , 23.2686° , 28.9988° , 29.5438° for 2:25 ratio, 15.4258° , 17.5811° , 21.5946° , 22.1286° , 22.6179° , 23.2695° , 29.0084° for 3:25 ratio, and 17.5430° , 17.8048° , 20.5391° , 20.6860° , 21.8042° , 22.2481° , 22.7660° , 23.5663° , 29.1780° for 4:25 ratio. Miller indices (h, k, l) values for 1:25 ratio were 100, 210 and 220; whereas 100, 200 and 220 for 2:25 ratio; 100, 210 and 220 for 3:25 ratio; and 100, 210 and 220 for 4:25 ratio. Different peaks confirmed that vincristine loaded nanoparticles were crystalline in nature and Miller Indices values further confirmed presence of nanoparticles in face centered cubic symmetry in all ratios. Such type of shifting in peaks has not been reported in literature and might be due to loading of vincristine in chitosan nanoparticles. There

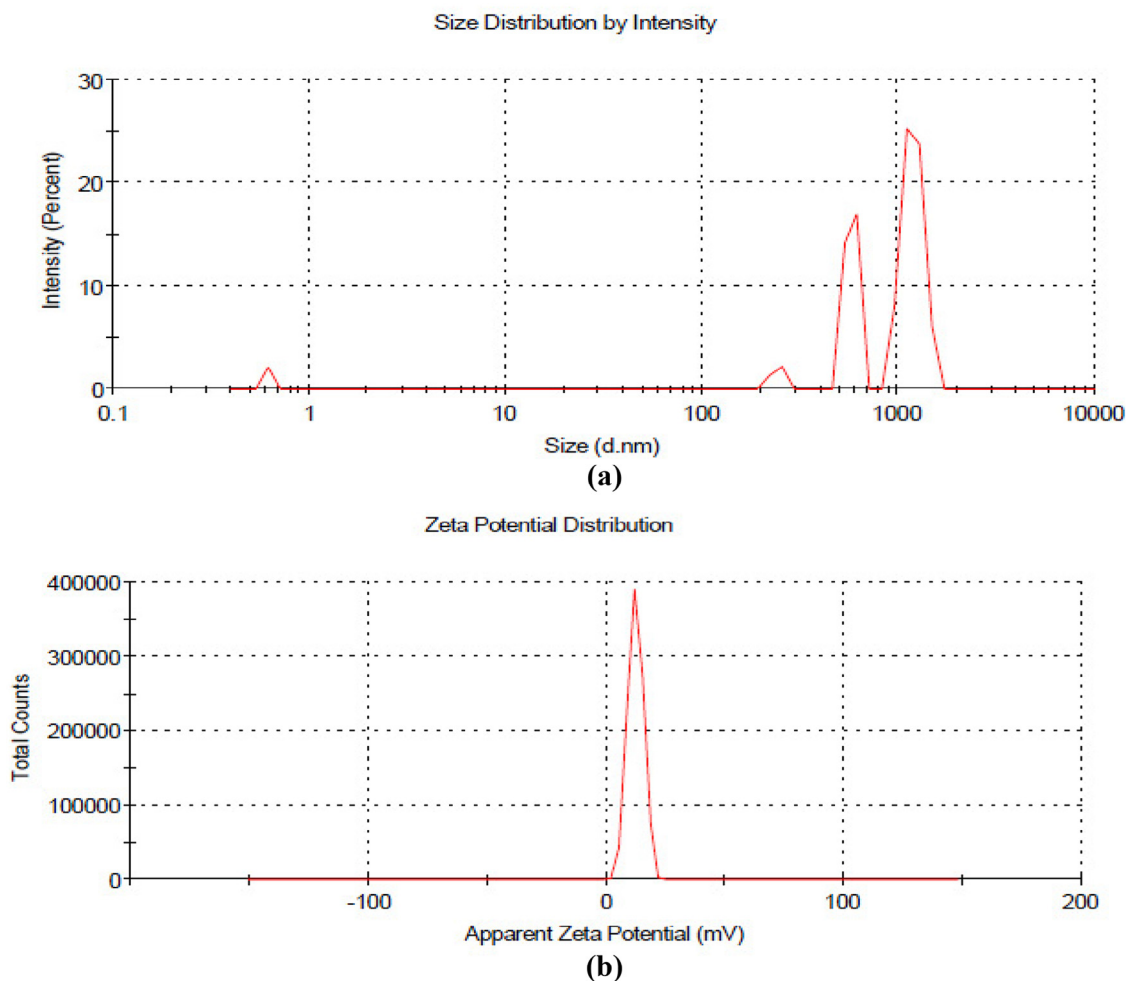


Fig. 7. Vincristine loaded folic acid–chitosan conjugated nanoparticles at a ratio of 4:25. (a) Average particle size and polydispersity index (b) zeta potential.

occurred no change in the symmetry of nanoparticles with increase in concentration of vincristine in folic acid–chitosan conjugated nanoparticles.

3.5.4. In vitro release study

As shown in Fig. 10, 1:25 formulation showed 25% of cumulative release of vincristine within 2 h and 50% in 4 h and there was no further release of the drug with the passage of time. In contrast formulation of 2:25 showed 2.3% release of vincristine within 2 h and subsequently 3.85, 5.38, and 6.15% release within 4, 6 and 8 h, respectively. Similarly, a formulation of 3:25 showed 3% release of vincristine within 2 h and for 4, 6, and 8 h the release was 10, 25, and 35%, respectively. Formulation 4:25 showed 3.07% release of vincristine within 2 h from folic acid–chitosan conjugated nanoparticles. It is therefore clear that 1:25 ratio was the best formulation that could release 50% of the loaded drug from folic acid–chitosan conjugated nanoparticles under *in vitro* conditions.

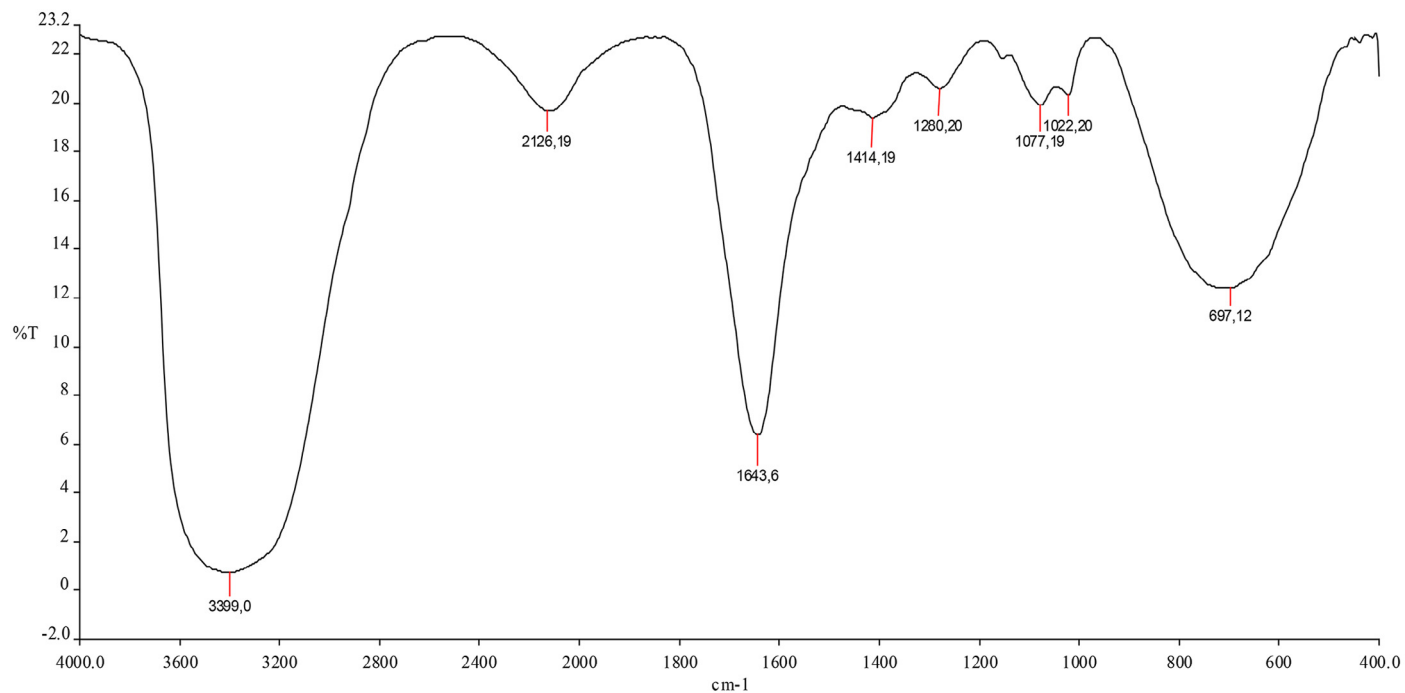
3.5.5. Scanning electron microscopy (SEM)

SEM images of the blank and vincristine loaded folic acid–chitosan conjugated nanoparticles are depicted in Fig. 11.

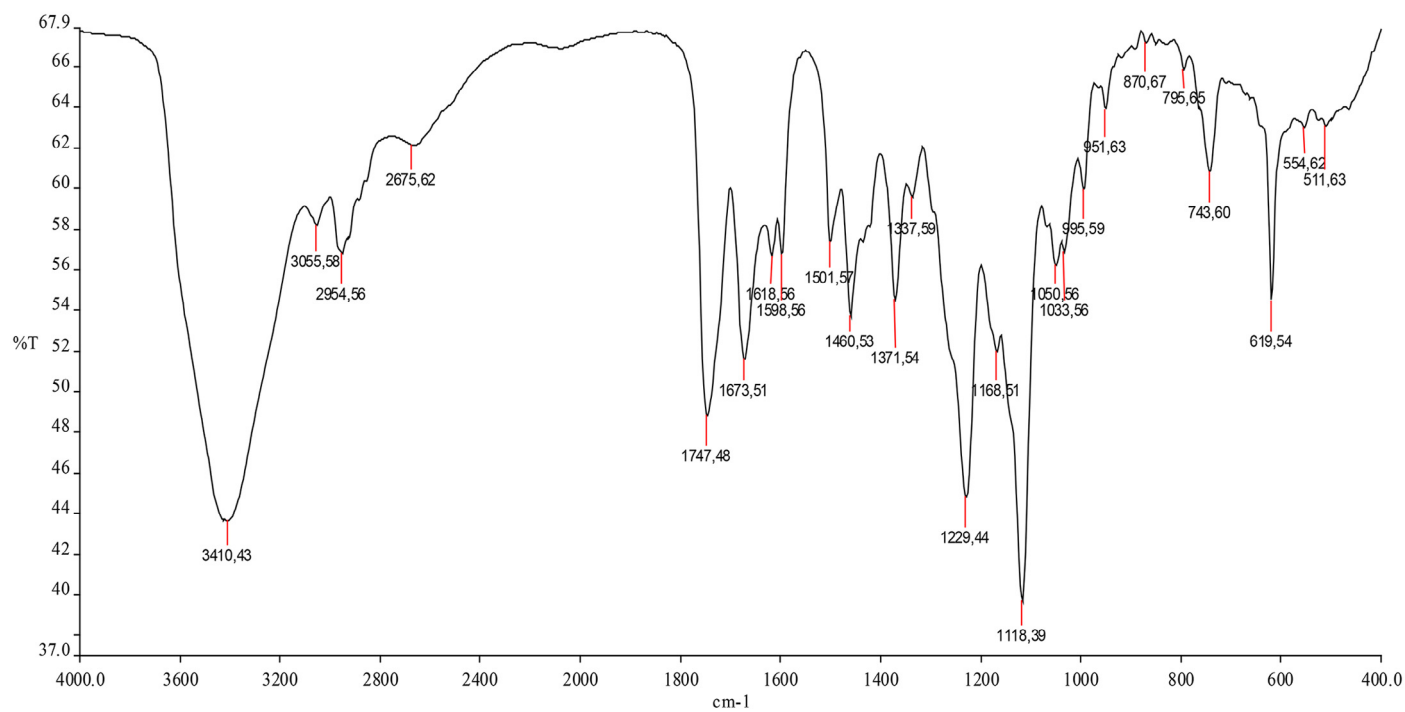
Different sized nanoparticles had spherical structure and rough surface. Earlier, spherical chitosan and gemcitabine loaded chitosan–pluronic® F nanoparticles have been reported [30]. Spherical shaped 5-fluorouracil loaded chitosan nanoparticles in different ratios were also examined [24]. On the contrary, well-formed spherical shaped, lomustine loaded chitosan-sodium tripolyphosphate and chitosan-sodium hexametaphosphate nanoparticles with smooth surface have also been observed [31].

3.5.6. Transmission electron microscopy (TEM)

TEM images of blank and the vincristine loaded nanoparticles are presented in Fig. 12. Blank nanoparticles were spherical in structure having a size of 200 nm without any contrast inside. Folic acid–chitosan conjugated nanoparticles in 1:25, 2:25, 3:25 and 4:25 ratios were spherical in structure with size ranging from 4.24 to 300 nm. These nanoparticles had granule like structures inside due to loading of vincristine in chitosan nanoparticles which confirmed loading of vincristine in folic acid–chitosan conjugated nanoparticles. This difference in average particle size measured with zeta sizer as compared to TEM

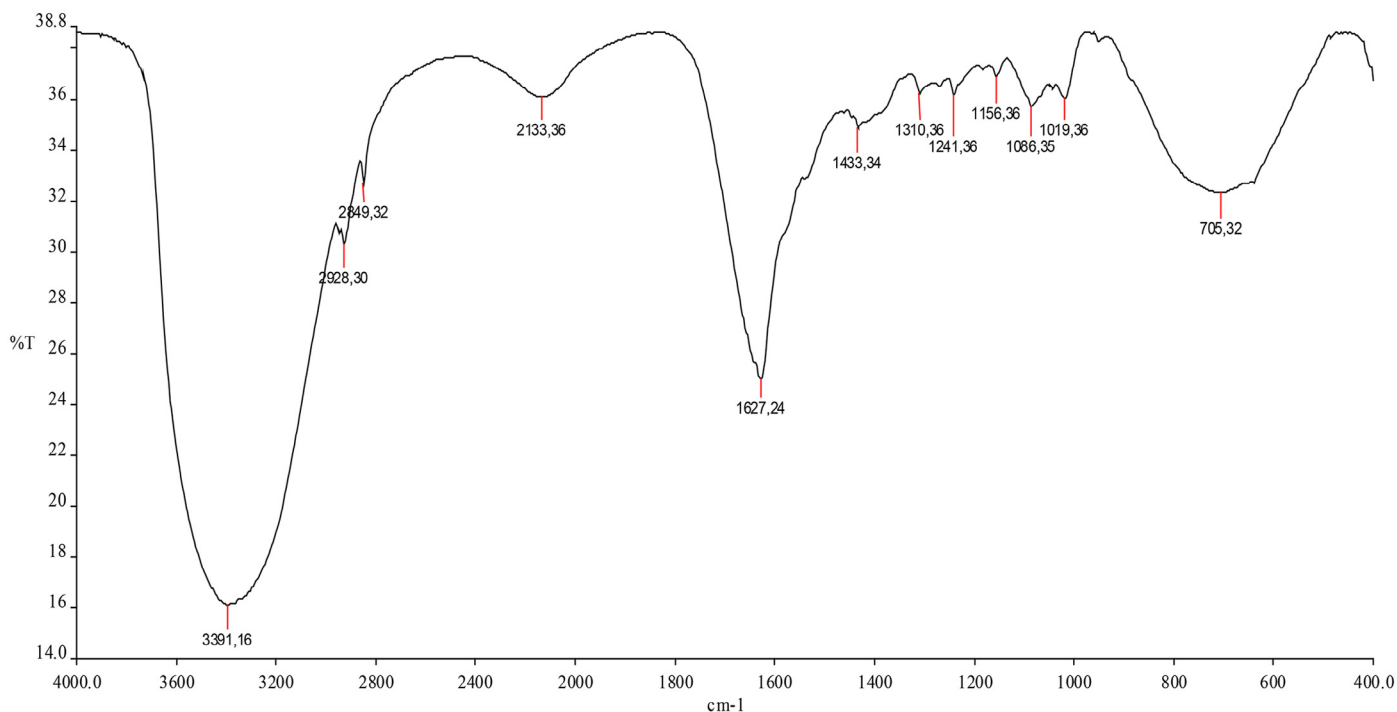


(a)

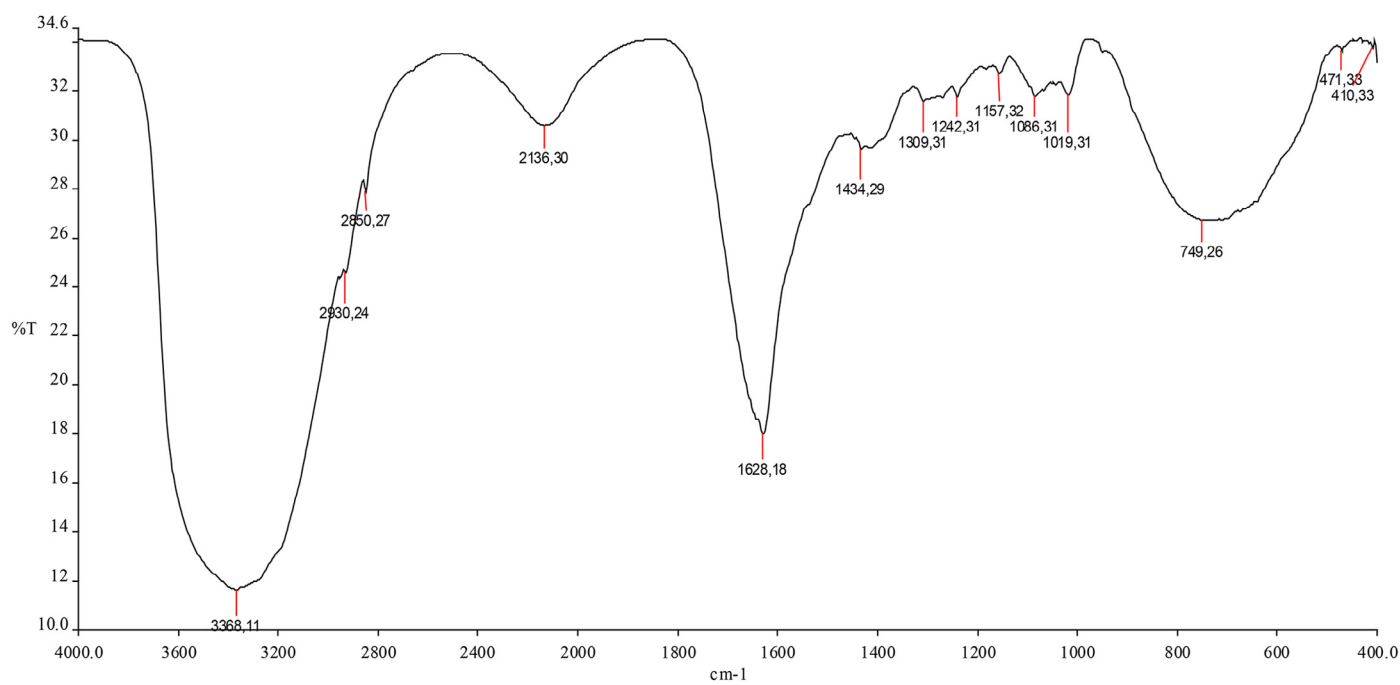


(b)

Fig. 8. FTIR spectra showing different functional groups: (a) blank nanoparticles, (b) vincristine and at different ratios (c) 1:25, (d) 2:25, (e) 3:25, (f) 4:25.



(c)



(d)

Fig. 8 (continued)

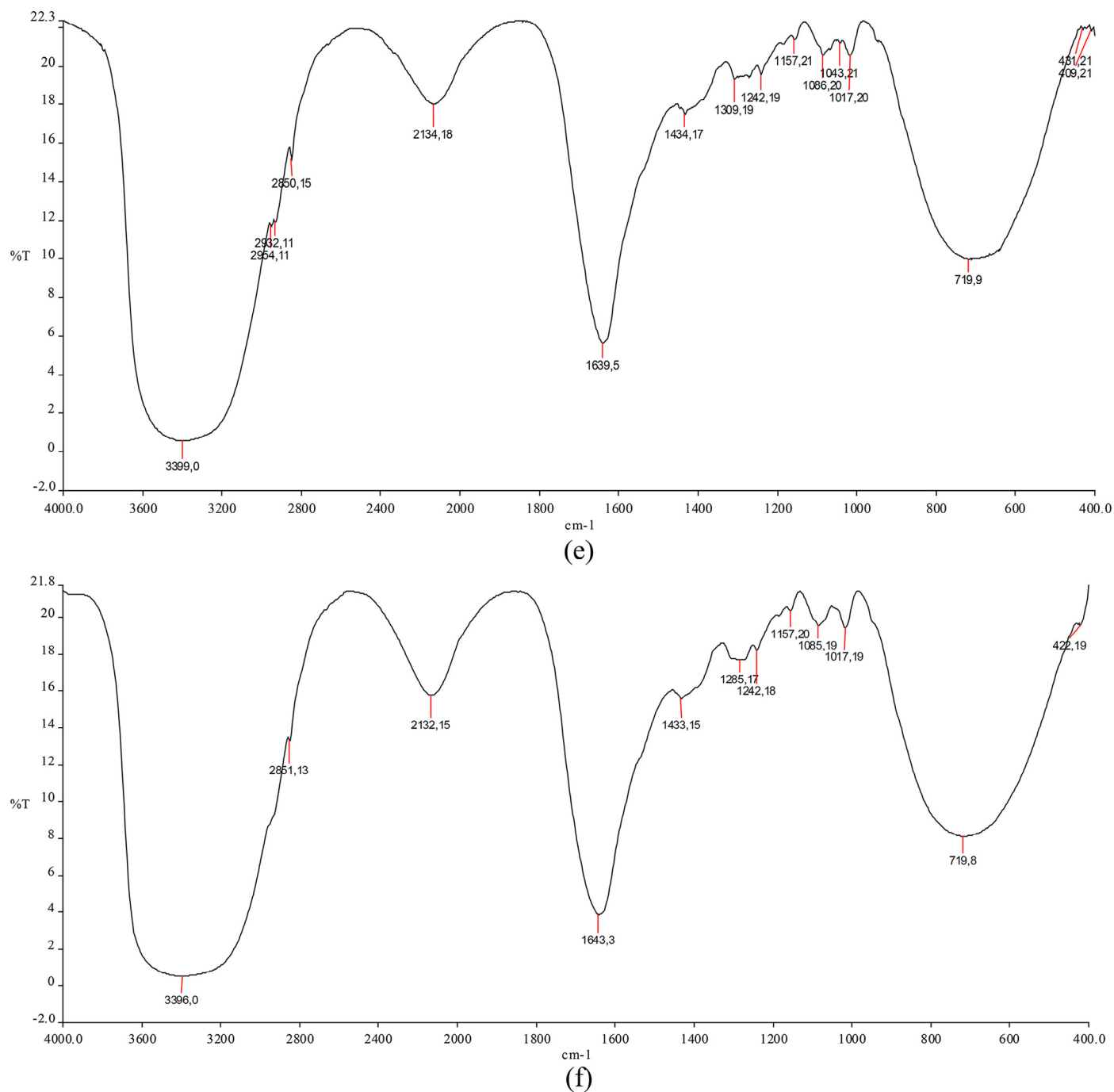


Fig. 8 (continued)

might be due to difference in sample preparation in both techniques. Earlier we [32] have used a different approach to synthesize spherical shaped silver nanoparticles ranging from 4.98 to 29 nm for enhanced antibacterial activity of streptomycin against some human pathogens. Spherical shaped, gefitinib and chloroquine loaded chitosan nanoparticles with size of 80.8 ± 9.7 nm to overcome the drug resistance have been scrutinized by Zhao et al. [33]. Mitoxantrone loaded folic acid–chitosan conjugated nanoparticles in size range of 39 nm–53 nm have been observed. Spherical shaped paclitaxel

loaded hydrophobically modified carboxymethyl chitosan nanoparticles for targeted delivery against mouse fibroblast NIH 3T3 and human cervical carcinoma (Hela) were synthesized earlier by Sahu et al. [34].

4. Conclusion

Folic acid–chitosan conjugated nanoparticles were synthesized by keeping folic acid–chitosan conjugate (25 ml) and sodium tripolyphosphate (5 ml) constant. Vincristine in different

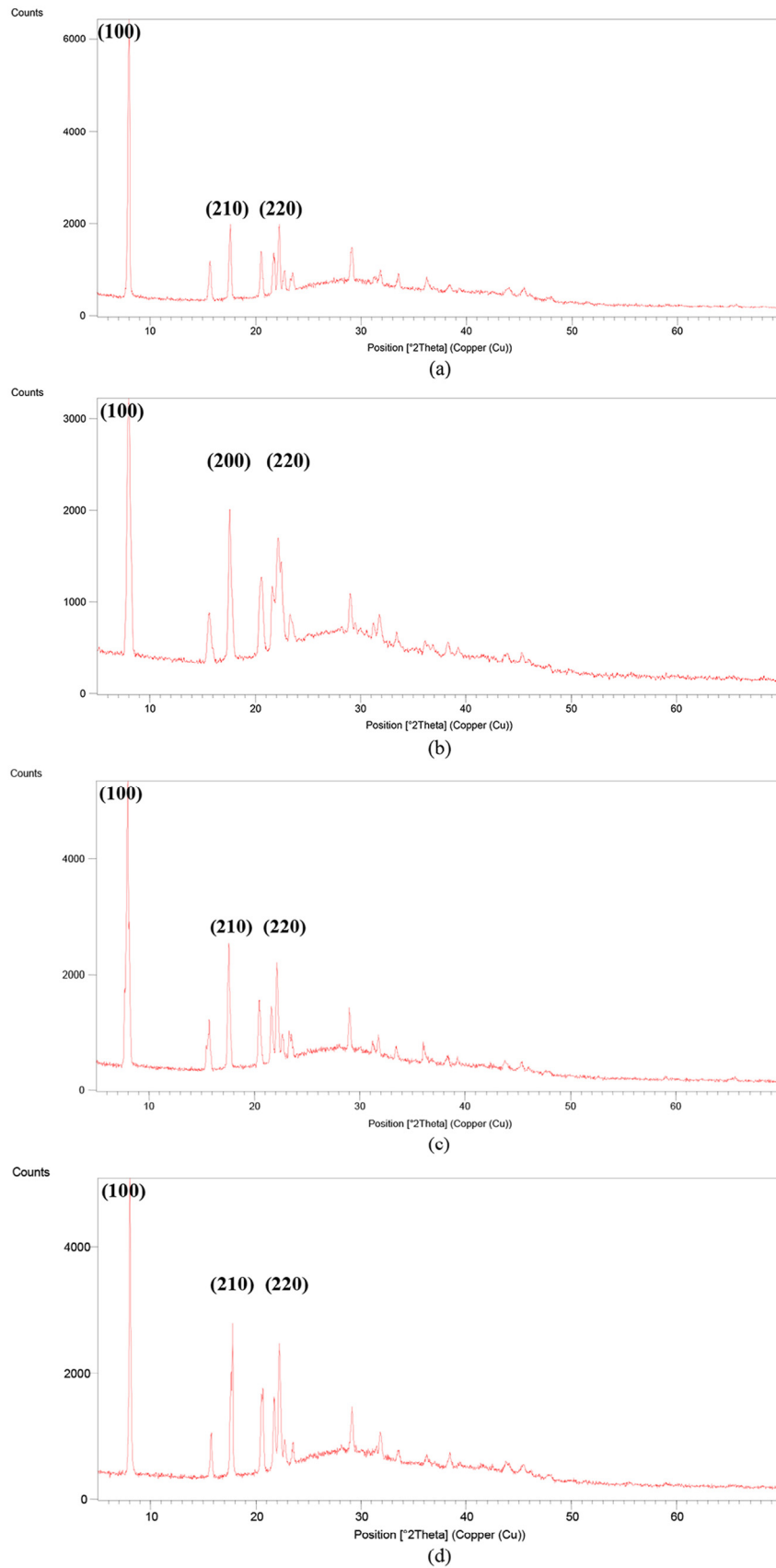


Fig. 9. XRD diffractogram with crystalline peaks of vincristine loaded folic acid–chitosan conjugated nanoparticles at different ratios: (a) 1:25, (b) 2:25, (c) 3:25, (d) 4:25.

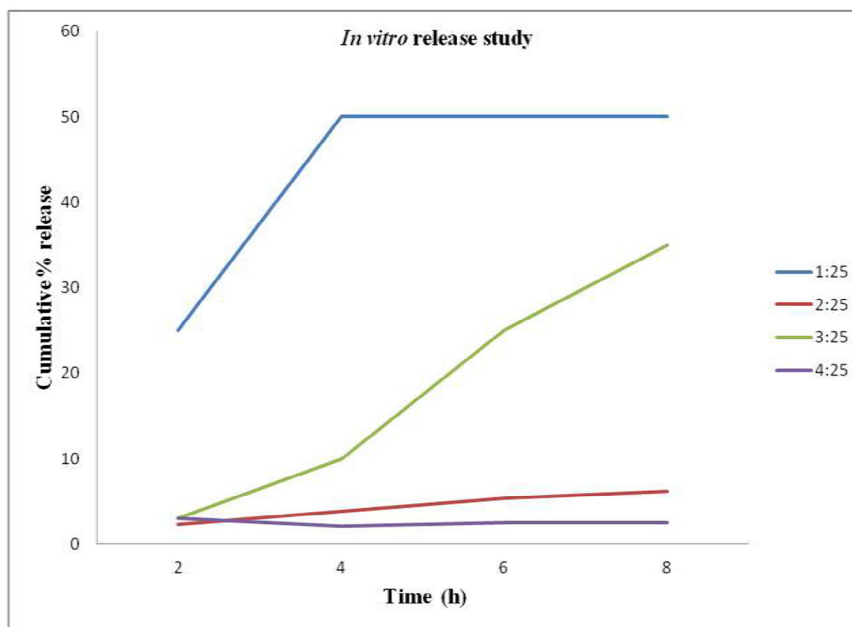


Fig. 10. *In vitro* release study of vincristine loaded FA-CS nanoparticles at pH 6.7.

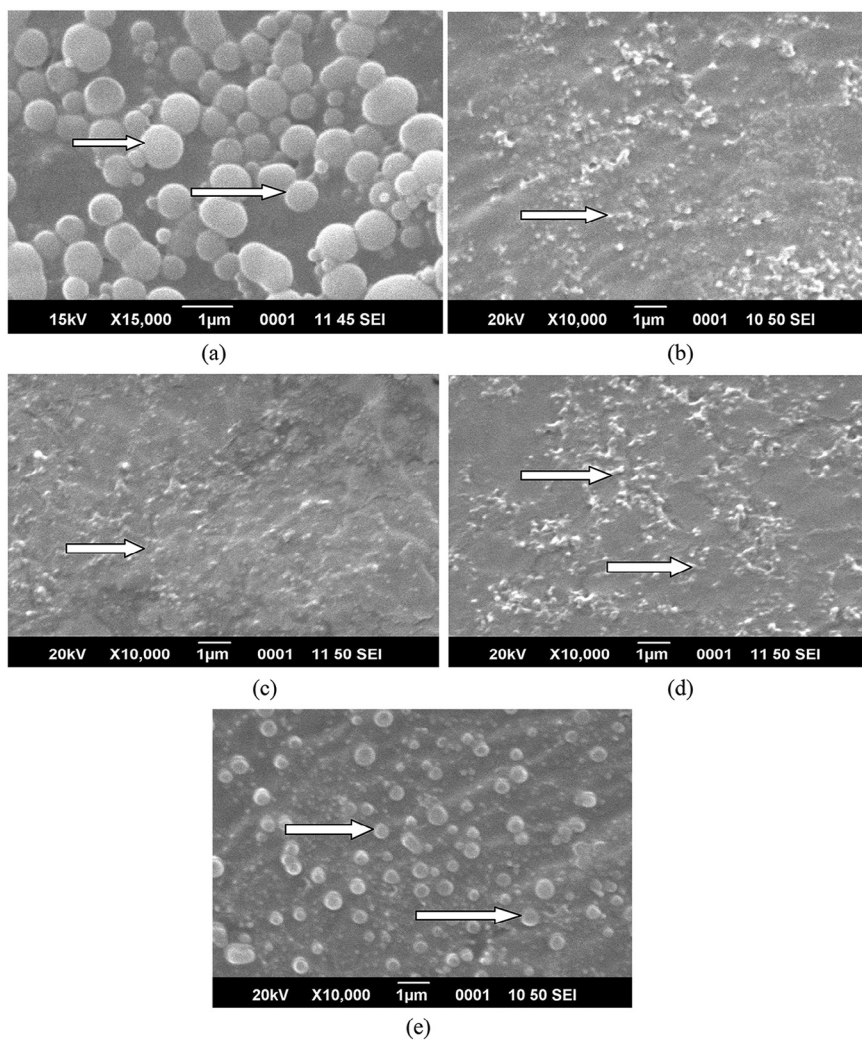


Fig. 11. SEM images of nanoparticles showing spherical shaped (a) blank and at different ratios (b) 1:25, (c) 2:25, (d) 3:25, (e) 4:25.

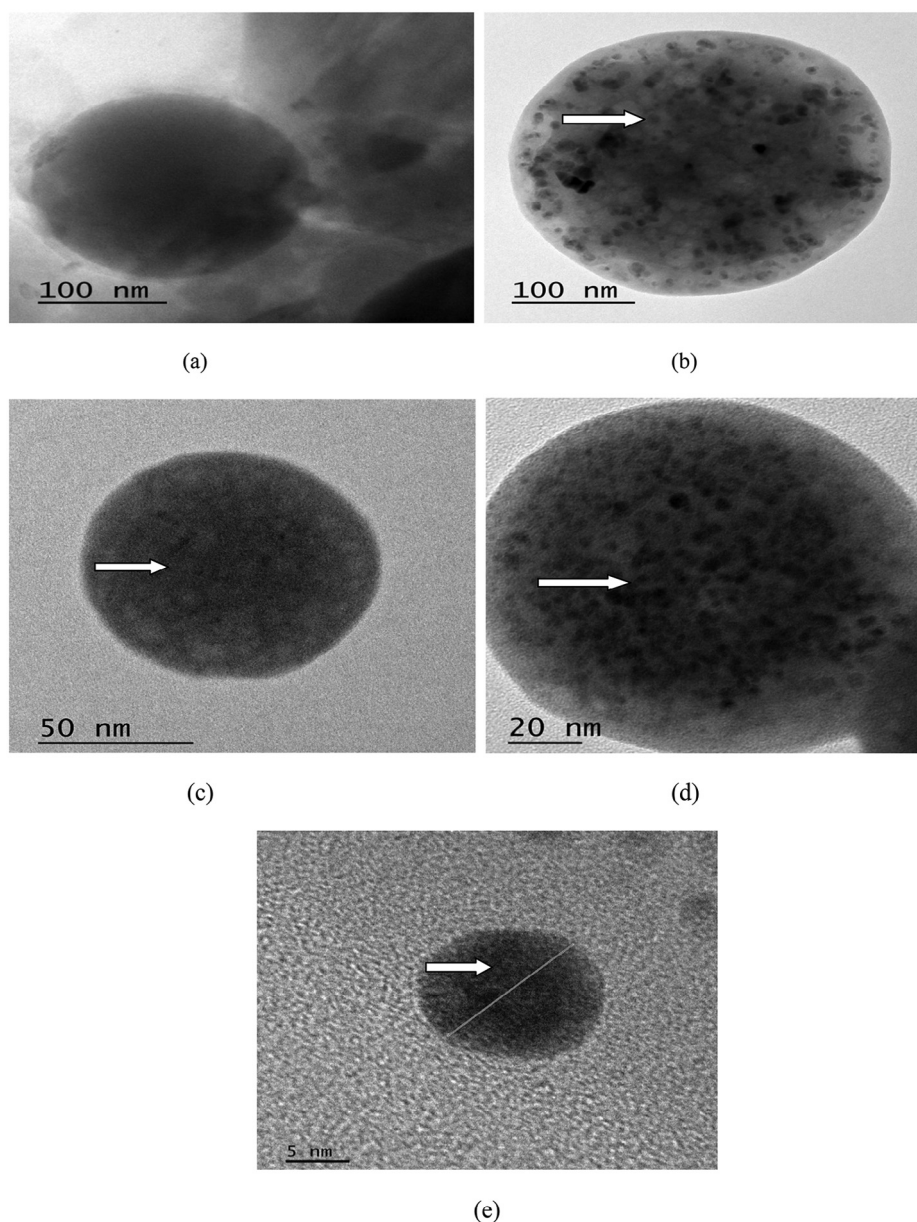


Fig. 12. TEM images of nanoparticles showing encapsulation of vincristine (a) blank and at different ratios (b) 1:25, (c) 2:25, (d) 3:25, (e) 4:25.

formulations [100 μ l (1:25), 200 μ l (2:25), 300 μ l (3:25), 400 μ l (4:25)] was loaded in folic acid–chitosan conjugated nanoparticles. Maximum encapsulation efficiency (%) and actual loading capacity (%) were 81.25 and 10.31, respectively and were observed for 4:25 formulation. Encapsulation of vincristine was confirmed with Fourier Transform Infrared Spectroscopy (FTIR) and Transmission Electron Microscopy (TEM). Scanning Electron Microscopy (SEM) revealed spherical structure and rough surface of nanoparticles. High temperature stability analysis showed the stability of vincristine loaded nanoparticles and were found to be highly stable at pH 7.2 and 7.6. Positive zeta potential also favors delivery of loaded vincristine in chitosan nanoparticles to cancer cells. But some modifications like pH and filtration of folic acid–chitosan conjugates in acetic acid are recommended to obtain nanoparticles with smaller and

uniform size with good polydispersity index. These results suggested that all formulations were important but 4:25 ratio was the best because of high encapsulation efficiency and loading capacity of vincristine in folic acid–chitosan conjugated nanoparticles and they can be used for targeted delivery to cancer cells with some modifications.

Acknowledgments

Authors acknowledge Central Instrumentation Laboratory and Sophisticated Analytical Instrumentation Facility, Panjab University, Chandigarh for assisting in FTIR and XRD analyses, respectively. Authors also would like to thank Sophisticated Test & Instrumentation Centre, Cochin University of Science and Technology, Cochin for help in Thermogravimetric

analysis, Differential Thermal Analysis, Differential Scanning Calorimetry, SEM and TEM. Authors also acknowledge Prof. Tibor Hianik, Department of Nuclear Physics and Biophysics, Faculty of Mathematics, Physics and Informatics, Comenius University, Bratislava, Slovak Republic for help in polydispersity index and zeta potential measurements. NK gratefully acknowledges Chaudhary Devi Lal University, Sirsa for awarding University Research Scholarship to carry out this work.

References

- [1] A.K. Garg, T.A. Buchholz, B.B. Aggarwal, Chemosensitization and radiosensitization of tumors by plant polyphenols, *Antioxid. Redox Signal.* 7 (2005) 1630–1647.
- [2] <http://www.druglib.com/activeingredient/vincristine/>.
- [3] M.A. Jordan, R.H. Himes, L. Wilson, Comparison of the effects of vinblastine, vincristine, vindesine, and vinepidine on microtubule dynamics and cell proliferation *in vitro*, *Cancer Res.* 45 (1985) 2741–2747.
- [4] M.J. Towle, K.A. Salvato, B.F. Wels, K.K. Aalfs, W. Zheng, B.M. Seletsky, et al., Eribulin induces irreversible mitotic blockade: implications of cell-based pharmacodynamics for *in vivo* efficacy under intermittent dosing conditions, *Cancer Res.* 71 (2011) 496–505.
- [5] C.D. Chiang, E.J. Song, V.C. Yang, C.C. Chao, Ascorbic acid increases drug accumulation and reverses vincristine resistance of human non-small-cell lung-cancer cells, *Biochem. J.* 301 (1994) 759–764.
- [6] Y.X. Yang, Z.Q. Xiao, Z.C. Chen, G.Y. Zhang, H. Yi, P.F. Zhang, et al., Proteome analysis of multidrug resistance in vincristine-resistant human gastric cancer cell line SGC7901/VCR, *Proteomics* 6 (2006) 2009–2021.
- [7] K. Kohno, J. Kikuchi, S. Sato, H. Takano, Y. Saburi, K. Asoh, et al., Vincristine-resistant human cancer KB cell line and increased expression of multidrug-resistance gene, *Jpn. J. Cancer Res.* 79 (1988) 1238–1246.
- [8] P.K. Vemula, J. Li, G. John, Enzyme catalysis: tool to make and break amygdalin hydrogelators from renewable resources: a delivery model for hydrophobic drugs, *J. Am. Chem. Soc.* 128 (2006) 8932–8938.
- [9] S. Salmaso, S. Bersani, A. Semenzato, P. Caliceti, New cyclodextrin bioconjugates for active tumour targeting, *J. Drug Target.* 15 (2007) 379–390.
- [10] P.W. Li, G. Wang, Z.M. Yang, W. Duan, Z. Peng, L.X. Kong, et al., Development of drug-loaded chitosan–vanillin nanoparticles and its cytotoxicity against HT-29 cells, *Drug Deliv.* 23 (2016) 30–35, doi:10.3109/10717544.2014.900590.
- [11] N. Liu, X.-G. Chen, H.-J. Park, C.-G. Liu, C.-S. Liu, X.-H. Meng, et al., Effect of MW and concentration of chitosan on antibacterial activity of *Escherichia coli*, *Carbohydr. Polym.* 64 (2006) 60–65.
- [12] B. Hu, C. Pan, Y. Sun, Z. Hou, H. Ye, X. Zeng, Optimization of fabrication parameters to produce chitosan-tripolyphosphate nanoparticles for delivery of tea catechins, *J. Agric. Food Chem.* 56 (2008) 7451–7458.
- [13] K.I. Jang, H.G. Lee, Stability of chitosan nanoparticles for l-ascorbic acid during heat treatment in aqueous solution, *J. Agric. Food Chem.* 56 (2008) 1936–1941.
- [14] K. Nagpal, S.K. Singh, D.N. Mishra, Chitosan nanoparticles: a promising system in novel drug delivery, *Chem. Pharm. Bull. (Tokyo)* 58 (2010) 1423–1430.
- [15] P. Sofia, B. Dimitrios, A. Konstantinos, K. Evangelos, G. Manolis, Chitosan nanoparticles loaded with dorzolamide and pramipexole, *Carbohydr. Polym.* 73 (2008) 44–54.
- [16] W.J. Guo, G.H. Hinkle, R.J. Lee, ^{99m}Tc-HyNIC-folate: a novel receptor-based targeted radiopharmaceutical for tumor imaging, *J. Nucl. Med.* 40 (1999) 1563–1569.
- [17] J. Ji, D. Wu, L. Liu, J. Chen, Y. Xu, Preparation, characterization, and *in vitro* release of folic acid-conjugated chitosan nanoparticles loaded with methotrexate for targeted delivery, *Polym. Bull.* 68 (2012) 1707–1720.
- [18] P. Calvo, C. Remunan Lopez, J.L. VilaJato, M.J. Alonso, Novel hydrophilic chitosan-polyethylene oxide nanoparticles as protein carriers, *J. Appl. Polym. Sci.* 63 (1997) 125–132.
- [19] E.S. Lee, K. Na, Y.H. Bae, Polymeric micelle for tumor pH and folate-mediated targeting, *J. Control. Release* 91 (2003) 103–113.
- [20] Z.P. Zhang, S.H. Lee, S.S. Feng, Folate-decorated poly(lactide-co-glycolide)-vitamin E TPGS nanoparticles for targeted drug delivery, *Biomaterials* 28 (2007) 1889–1899.
- [21] D. Lee, R. Lockey, S. Mohapatra, Folate receptor-mediated cancer cell specific gene delivery using folic acid-conjugated oligochitosans, *J. Nanosci. Nanotechnol.* 6 (2006) 2860–2866.
- [22] <http://www.science-and-fun.de/tools/>.
- [23] Y. Pan, Y.J. Li, H.Y. Zhao, J.M. Zheng, H. Xu, G. Wei, et al., Bioadhesive polysaccharide in protein delivery system: chitosan nanoparticles improve the intestinal absorption of insulin *in vivo*, *Int. J. Pharm.* 249 (2002) 139–147.
- [24] S.S. Saravanabhavan, R. Bose, S. Skylab, S. Dharmalingam, Fabrication of chitosan/TPP nanoparticles as a carrier towards the treatment of cancer, *Int. J. Drug Deliv.* 5 (2013) 35–42.
- [25] R. Panwar, A.K. Sharma, M. Kaloti, D. Dutt, V. Pruthi, Characterization and anticancer potential of ferulic acid-loaded chitosan nanoparticles against ME-180 human cervical cancer cell lines, *Appl. Nanosci.* 6 (2016) 803–813, doi:10.1007/s13204-015-0502-y.
- [26] J.F. Duan, J. Du, Y.B. Zheng, Preparation and drug-release behavior of 5-fluorouracil-loaded poly(lactic acid-4-hydroxyproline-polyethylene glycol) amphipathic copolymer nanoparticles, *J. Appl. Polym. Sci.* 103 (2007) 2654–2659.
- [27] W. Wang, C. Tong, X. Liu, T. Li, B. Liu, W. Xiong, Preparation and functional characterization of tumor-targeted folic acid-chitosan conjugated nanoparticles loaded with mitoxantrone, *J. Cent. South Univ.* 22 (2015) 3311–3317.
- [28] Y.M. Xu, Y.M. Du, Effect of molecular structure of chitosan on protein delivery properties of chitosan nanoparticles, *Int. J. Pharm.* 250 (2003) 215–226.
- [29] D. Jeevitha, A. Kanchana, Evaluation of chitosan/poly (lactic acid) nanoparticles for the delivery of piceatannol, an anti-cancer drug by ionic gelation method, *Int. J. Chem. Environ. Biol. Sci.* 2 (2014) 12–16.
- [30] H. Hosseinzadeh, F. Atyabi, R. Dinarvand, S.N. Ostad, Chitosan–pluronic nanoparticles as oral delivery of anticancer gemcitabine: preparation and *in vitro* study, *Int. J. Nanomed.* 7 (2012) 1851–1863.
- [31] A. Mehrotra, R.C. Nagarwal, J.K. Pandit, Fabrication of lomustine loaded chitosan nanoparticles by spray drying and *in vitro* cytostatic activity on human lung cancer cell line L132, *J. Nanomed. Nanotechnol.* 1 (2010) 103, doi:10.4172/2157-7439.1000103.
- [32] R.K. Salar, P. Sharma, N. Kumar, Enhanced antibacterial activity of streptomycin against some human pathogens using green synthesized silver nanoparticles, *Res. Eff. Technol.* 1 (2015) 106–115.
- [33] L. Zhao, G. Yang, Y. Shi, C. Su, J. Chang, Co-delivery of Gefitinib and chloroquine by chitosan nanoparticles for overcoming the drug acquired resistance, *J. Nanobiotechnol.* 13 (2015) 57, doi:10.1186/s12951-015-0121-5.
- [34] S.K. Sahu, S. Maiti, T.K. Maiti, S.K. Ghosh, P. Pramanik, Hydrophobically modified carboxymethyl chitosan nanoparticles targeted delivery of paclitaxel, *J. Drug Target.* 19 (2011) 104–113.